Int. J. Electrochem. Sci., 11 **(2016)** 2778 - 2789

International Journal of
ELECTROCHEMICAL
SCIENCE
www.electrochemsci.org

Electrochemical Sensor for Ultrasensitive Determination of Bisphenol A based on Gold Nanoparticles/β-cyclodextrin Functionalized Reduced Graphene Oxide Nanocomposite

Yang Yun[1,2,*]

[1] Department of Application Chemistry, College of Science, Tianjin University of Commerce, Tianjin, 300134, P. R. China
[2] Tianjin Key Laboratory for Prevention and Control of Occupational and Environmental Hazards，Logistics University of PAPF Tianjin,300162, P. R. China.
[*]E-mail: yyun@tjcu.edu.cn

Received: 7 January 2016 / *Accepted:* 29 January 2016 / *Published:* 1 March 2016

In this work, an electrochemical sensor based on a β-cyclodextrin functionalized reduced graphene oxide/gold nanoparticles (β-CD/RGO/Au) composite modified glassy carbon electrode (GCE) was proposed for the ultrasensitive detection of bisphenol A (BPA). The β-CD/RGO/Au nanocomposite was synthesized by a microwave heating method followed by an electrodeposition process. The prepared nanocomposite was carefully characterized by FTIR, Raman spectroscopy, UV-vis spectroscopy, SEM, EDX and XRD. The electrocatalytic oxidation of BPA on the modified GCE was investigated by cyclic voltammetry (CV) and differential pulse voltammetry (DPV). The results showed that the β-CD/RGO/Au modified GCE could effectively enhance the electrochemical detection performance towards oxidation of BPA due to the synergetic effects of RGO and Au NPs with supramolecular recognition capability of β-CD. The proposed sensor exhibited excellent linear relationship between the detection current and BPA concentration in the range from 0.01 to 50 μM. The detection limit was estimated as 0.003 μM (S/N = 3). Moreover, the proposed BPA sensor has also been successfully used for determining BPA in various real samples.

Keywords: Graphene; Gold nanoparticle; Electrochemical; Electrodeposition; Bisphenol A

1. INTRODUCTION

Bisphenol A (BPA, $(CH_3)_2C(C_6H_4OH)_2$) is an important industrial chemical for the production of epoxy resins and polycarbonate plastics, which have been widely used as food containers and water bottles [1]. It is also a typical endocrine disrupting compound which can mimic estrogen and has been

associated with a series of adverse health effects [2-5]. Besides human health, BPA also could impact the environment. Several report claimed that the BPA can migrate into the environment through manufacturing and degradation process of plastics [6, 7]. Therefore, it is important to develop a sensitive, quick and reliable method for determining BPA in different type of samples. Up to now, a series of analytical technologies have been developed for BPA determination, including high-performance liquid chromatography (HPLC) [8-11], enzyme-linked immunosorbent assay (ELISA) [12, 13] and gas chromatography-mass spectrometry (GC–MS) [14, 15]. Although these methods are highly capable for determining BPA at low content, but they usually have drawbacks such as time-consuming, expensive and required skilled technician. Therefore, they cannot be directly used for real applications. In order to overcome these drawbacks, electrochemical method have attracted more attentions due to its sensitivity, accuracy, lower cost and simplicity [16-32].

BPA is an electrochemically active subtance, however, it is irreversible for direct electrochemical oxidation of BPA at bare electrodes and high overpotential is required. Moreover, oxidation of BPA on bare electrode could result oxidation products that foul the electrode [33]. Therefore, electrode surface modification has been adopted to overcome these problems. So for, different types of materials such as carbon nanotubes [34-38], mesoporous silica [39], CoTe quantum dots [40], ZnO nano tetrapods [41] and Ni(II) tetraaminometallophthalocyanine polymer [42] were used for electrochemical determination of BPA. However, the fabrication of novel electrode modified materials with quick response, excellent conductivity, good sensitivity and high stability remains a challenge.

Graphene is a two-dimensional single-atom-thick conjugated carbon network, has received a great attention of attention in since it has been discovered in 2004 [43], due to its extraordinary properties, graphene became an outstanding candidate for electrode surface modification for specific target molecule detection. However, preparation of dispersive graphene is challenging as graphene is known to have poor dispersibility in solvents. In order to solve this problem, β-cyclodextrin (β-CD), a cyclic polysaccharide composed of seven glucose molecules, has been studied for functionalizing graphene [44]. Studied also showed that β-CD can bind many kinds of organic, inorganic and biological molecules into their cavities to form stable host-gust inclusion complexes [45, 46], which provide an excellent opportunity for fabricating electrochemical sensor. On the other hand, gold nanoparticles (Au NPs) are widely used nanomaterials for the fabrication of electrochemical biosensors because they can provide suitable microenvironments for immobilization of biomolecules with excellent electrocatalytic property [47-51].

In this work, we synthesized an aqueous suspension of reduced graphene oxide (RGO) by using β-CD as dispersants through a simple a microwave heating method. Subsequently, a sensitive electrochemical sensor for BPA detection was fabricated by electrodeposition of Au NPs on the β-CD/RGO modified glassy carbon electrode (GCE). The result β-CD/RGO/Au nanocomposite was characterized by a series of techniques. Due to the excellent electric conductivity of RGO, synergistic effect between RGO and Au NPs, and the competitive host–guest interaction between β-CD and BPA molecules, our proposed sensor exhibited excellent electrocatalytic activity towards oxidation of PBA with wide linear range and low detection limit. In addition, the proposed sensor was applied to determine BPA in various real samples.

2. EXPERIMENTS

2.1 Chemicals and materials

Bisphenol A (BPA, 97%), synthetic graphite (average particle diameter <20 μm), $HAuCl_4 \cdot 3H_2O$, phenol, hydroxyphenol, 4-nitrophenol, 2,4-dinitrophenol, pyrocatechol, dioctyl hthalate and β-CD were purchased from Sigma-Aldrich. Other chemicals were of analytical reagent grade and used without further purification. Phosphate buffer solution (PBS) was prepared by mixing 0.1 M KH_2PO_4 and K_2HPO_4 solution to appropriate pH. Milli-Q water (18.2 MΩ cm) was used throughout the experiments.

2.2 Synthesis of β-CD/RGO/Au nanocomposite

Graphene oxide (GO) was prepared with the modified Hummers method with little modification [52, 53]. β-CD/RGO was prepared by a microwave heating method according to the literature with some modifications [54]. Briefly, GO aqueous dispersion (0.5 mg/mL, 5 mL) was mixed with β-CD aqueous solution (1 mg/mL, 5 mL) by half hour sonication. The pH value of the mixed solution was adjusted to 12.0. Then, the mixed solution was heated for 5 minutes in a household microwave oven for GO reduction and surface functionalization. Black sediment was collected by 3 times centrifugation (10000 rmp, 10 min) followed by water wash. The β-CD/RGO nanocomposite was obtained after drying in an oven at 70°C for 12 h. For electrodeposition of Au NPs on β-CD/RGO nanocomposite, a GCE was polished with alumina-water slurry followed by rinsing with ethanol and water. 5 μL of β-CD/RGO nanocomposite dispersion (1 mg/mL) was dropped onto the GCE and dried at the room temperature. Next, electrochemical deposition of Au NPs on GCE was performed in 0.5 M H_2SO_4 solution containing 1% $HAuCl_4$ using chronoamperometry at an applied potential of −0.2 V for 60s (A platinum wire was used as the auxiliary electrode and an Ag/AgCl (3M KCl) as the reference electrode). Au NPs were also electrodeposited onto hydrazine reduced graphene oxide modified GCE using a similar method and denoted as RGO/Au. Following parameters were used for CV scan: 0.1 M PBS, pH 7, scan rate: 50 mV/s, scan potential range: 0.2─0.9 V. For DPV analysis, following parameters were used: 0.1 M PBS, pH 7, scan range: 0.2−0.9 V, amplitude: 50 mV.

3. RESULTS AND DISCUSSION

3.1 Characterization of β-CD/RGO/Au nanocomposite

FTIR was used for analysing the surface functionalization performance of GO. Figure 1A shows the FTIR spectra of GO, β-CD and β-CD/RGO/Au. The FTIR spectrum of GO shows peaks located at 1708 cm^{-1}, 1590 cm^{-1}, 1396 cm^{-1} and 1022 cm^{-1}, corresponding to the C═O stretching of COOH groups, C=C vibrations, C─OH stretching vibrations and C─O vibrations from alkoxy groups, respectively [55-57]. After microwave treatment with β-CD, the intensities of these peaks are significantly decreased or even dispersed, suggesting the β-CD could serve as a reduce agent for GO

reduction. As shown in the figure, the spectrum of β-CD/RGO/Au displays typical β-CD characteristic peaks of C=C conjugation at about 1632 cm^{-1}, CH_n stretching vibrations at 2924 cm^{-1}, O—H bending vibrations at 1138 cm^{-1} and the coupled C—O/C—C stretching at 1025 cm^{-1}, indicating the RGO sheets have been successfully functionalized by β-CD [58-60].

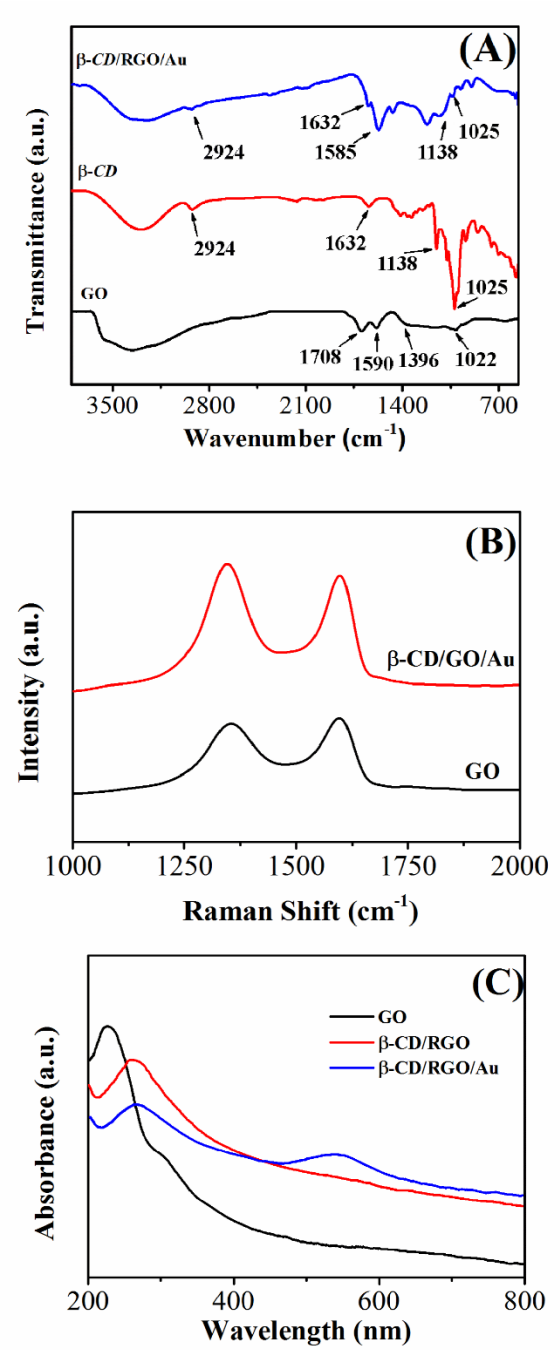

Figure 1. (A) FTIR spectra of GO, β-CD and β-CD/RGO/Au. (B) Raman spectra of GO and β-CD/RGO/Au. (C) UV-vis spectra of GO, β-CD/RGO and β-CD/RGO/Au.

Due to the high sensitivity to electronic structure change of carbon materials, Raman scattering was used for further confirm the reduction of GO. As shown in Figure 1B, the spectra of GO and β-CD/RGO/Au both show two characteristic peaks at 1570 and 1340 cm^{-1} [61]. The intensity ratio

between D band and G band (I_D/I_G) is found to be increased in β-CD/RGO/Au nanocomposite with compare to GO which confirm the removal of oxygen containing functional groups and the decrease of the average size of the sp^2 domains constructed in the RGO [62, 63].

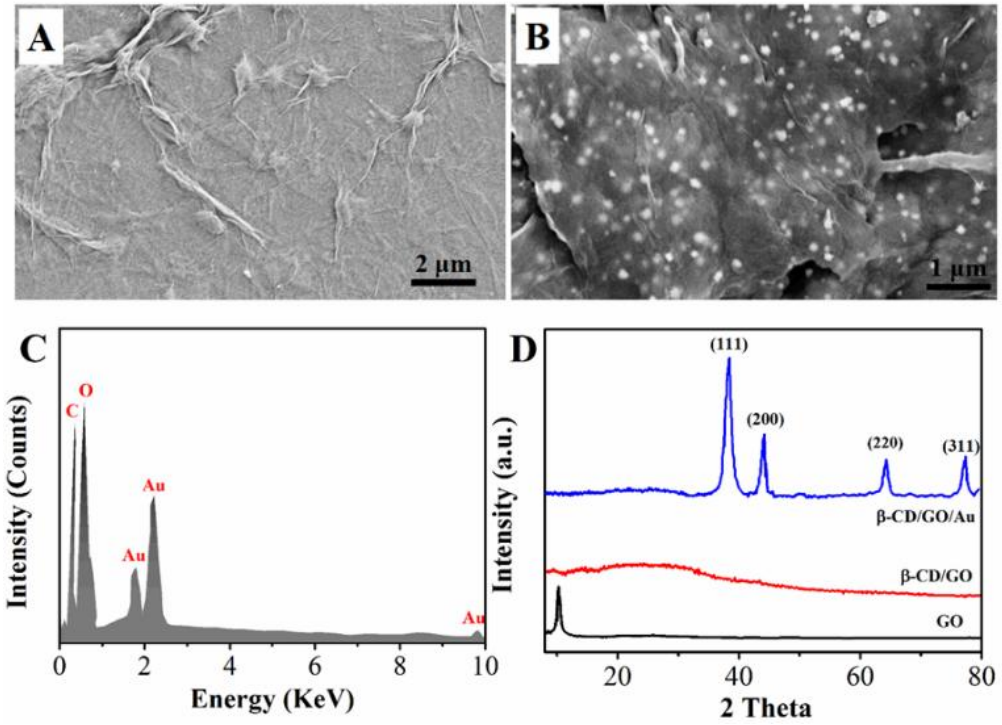

Figure 2. SEM images of (A) β-CD/RGO and (B) β-CD/RGO/Au. (C) EDX spectrum of β-CD/RGO/Au. (D) XRD patterns of GO, β-CD/RGO and β-CD/RGO/Au.

Figure 1C shows the UV-vis spectra of GO, β-CD/RGO and β-CD/RGO/Au. The spectrum of GO displays a maximum absorption peak centered at 226 nm and a shoulder peak at about 315 nm, which assign to the π─π* transitions of aromatic C─C bonds and n─π* transitions of C=O bonds [64]. After microwave treatment with β-CD, the absorption peak of GO dispersion at 226 nm gradually red-shifts to 266 nm and the shoulder absorption peak disappeared, indicating the GO has been reduced. Moreover, the spectrum of β-CD/RGO/Au also exhibits a new absorption peak at about 545 nm, corresponding to the surface plasmon absorption of gold NPs, which confirm the successful electrodeposition of Au NPs [65].

The surface morphology of the samples were subsequently observed by SEM. Figure 2A-B display the typical SEM images of β-CD/RGO and β-CD/RGO/Au nanocomposites. As shown in Figure 2A, β-CD/RGO displays a flake-like shape of graphene. Particularly, a wrinkled topology is observed in the SEM characterization due to the well dispersity of the sample. For β-CD/RGO/Au nanocomposite, it can be seen that Au NPs were uniformly decorated on the β-CD/RGO with an average size of 60 nm (based on more than 200 Au NPs). EDX characterization was applied to obtain elements information about β-CD/RGO/Au nanocomposite (Figure 2C). The spectrum presents the only existence of C, O and Au, suggesting the formation of the nanocomposite with high purity.

The crystalline information of GO, β-CD/RGO and β-CD/RGO/Au nanocomposite was characterized by XRD. As shown in the Figure 3D, it can be seen that the pure GO exhibits a characteristic (001) peak at 11.0° with a *d*-spacing value of 0.81 nm [66]. However, the disappearance of the (0 0 1) peak in β-CD/RGO suggest the successful reduction of GO and an appearance of a broad peak centred at 23.0°, indicating the presence of stacked graphene layers of RGO [67]. In β-CD/RGO/Au nanocomposite, the diffraction peaks at 38.3°, 43.6°, 63.5° and 76.9° are consistent with the (111), (200), (220) and (311) crystal faces of (fcc) Au NPs, respectively (JCPDS 4-0783).

The electrochemical properties of different modified electrodes were investigated using $K_3[Fe(CN)_6]$ as probes. As expected, the bare GCE shows an obvious redox peaks. Compared with the bare GCE, the redox current of $[Fe(CN)_6]^{3-/4-}$ at RGO/Au, β-CD/RGO and β-CD/RGO/Au modified GCEs are increased clearly, indicating the surface modifications used in our study can significantly enhance the conductivity of the electrode and facilitating the electron transfer. Among them, β-CD/RGO/Au modified GCE shows the highest current response, suggesting β-CD/RGO/Au could consider as an excellent modifier candidate for enhancing the performance of the electrode.

3.2 Electrochemical behavior of BPA at β-CD/RGO/Au modified electrodes

Figure 3A shows the voltammetric response (three electrodes system, scan rate: 50 mV/s, scan potential range: 0.2─0.9 V) of different electrodes towards oxidation of 0.5 mM BPA. At bare GCE, a small oxidation peak is observed at the potential of 0.59 V with a peak current of 9.61 μA. While at β-CD/RGO modified GCE, an oxidation peak with peak current about 47.31 μA is observed at 0.66 V. This current response enhancement could ascribe to the excellent conductivity and high surface area of β-CD/RGO nanocomposite. However, the oxidation potential shifts positively, which could against the practical application by the other interference species been oxidized in high potential range. In terms of RGO/Au modified GCE, the oxidation peak is observed at the potential of 0.56 V with a peak current of 36.67 μA. On the other hand, the β-CD/RGO/Au modified GCE gives a relatively big oxidation peak at 0.52 V with current of 82.23 μA, which is approximately 8.5 times for bare GCE, 2.2 times for RGO/Au modified GCE and 1.7 times for β-CD/RGO modified GCE. The enhancement of current response and lower the overpotential of BPA oxidation in β-CD/RGO/Au modified GCE could ascribe to the high specific surface area, the excellent electrocatalytic property and the synergistic effect between β-CD functionalized RGO sheets and Au NPs.

Figure 3B shows the CVs of the oxidation of 0.5 mM BPA at β-CD/RGO/Au modified GCE with different scan rates. The results shows that the oxidation peak current increases gradually with the increase of scan rate in the ranged from 20 to 200 mV/s. A linear relationship is obtained between the peak currents and the square root of scan rates (Figure 3C), indicating the oxidation of BPA on β-CD/RGO/Au modified GCE is a typical diffusion-controlled process.

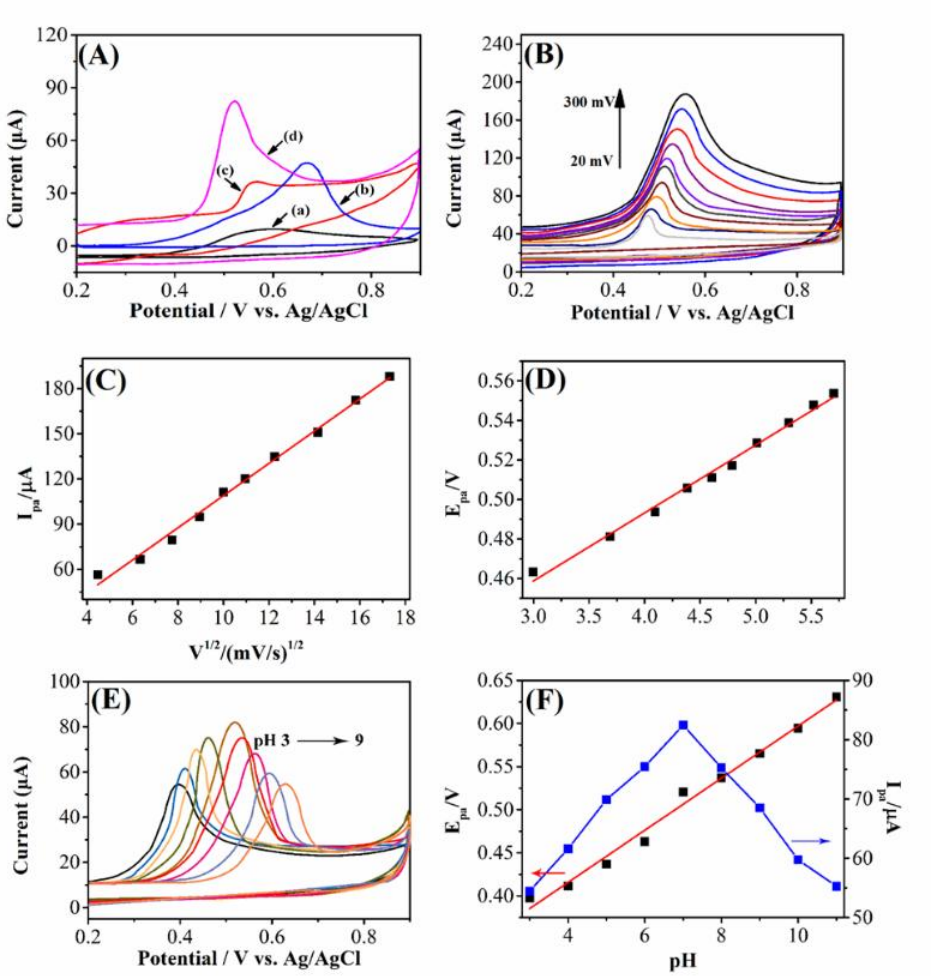

Figure 3. (A) CVs of bare (a) GCE, (b) β-CD/RGO (c) RGO/Au and (d) β-CD/RGO/Au modified GCEs in 0.1 M PBS (pH 7.0) containing 0.5 mM BPA. Scan rate: 50 mV/s. (B) CVs of β-CD/RGO/Au modified GCE in 0.5 mM BPA (PBS = 7.0) at different scan rates (20, 40, 60, 80, 100, 120, 150, 200, 250, 300 mV/s). (C) The plot for the dependence of peak current on the square root of scan rate. (D) The relationship between E_{pa} and lnv. (E) CV of β-CD/RGO/Au modified GCE in 0.5 mM BPA at different pH conditions. Scan rate: 50 mV/s. (F) Effect of pH on the oxidation current and oxidation potential.

This is consistent with reported work of others [19, 20, 68]. The linear regression equation can be represented as: I_{pa} (μA) = 10.693 $v^{1/2}$ (mV/s) + 2.034 (R^2 = 0.993). On the other hand, the anodic peak potential shifts positively when the scan rate increases. A linear relationship is obtained between the oxidation potentials and the logarithm of scan rates (Figure 3D), indicating the electrochemical reaction is irreversible. The linear regression equation can be represented as: E_{pa} (V) = 0.03187 lnv (mV/s) + 0.36825 (R^2 = 0.989). Based on this linear equation, the relationship between the E_{pa} and v can be expressed as follows by Laviron [69, 70]:

$$E_{pa} = E^0 + (RT/\alpha nF)\ln(RTk^0/\alpha nF) + (RT/\alpha nF)\ln v$$

Where E^0 is the formal redox potential; R is the gas constant; α is the electron transfer coefficient; F is the Faraday's constant and k^0 is the standard heterogeneous rate constant of the

reaction. As the slope of E_{pa} versus ln v is 0.03187, the αn value can be easily calculated as 1.3214. Then, the α can be determined as follow:

$$E_{pa/2} - E_{pa} = 1.875(RT/\alpha F)$$

α has been calculated as 0.5741. Therefore, the total number of electrons involved in the oxidation of BPA is found equal to 2, which is in good agreement with previous reports [16, 17, 19, 71, 72].

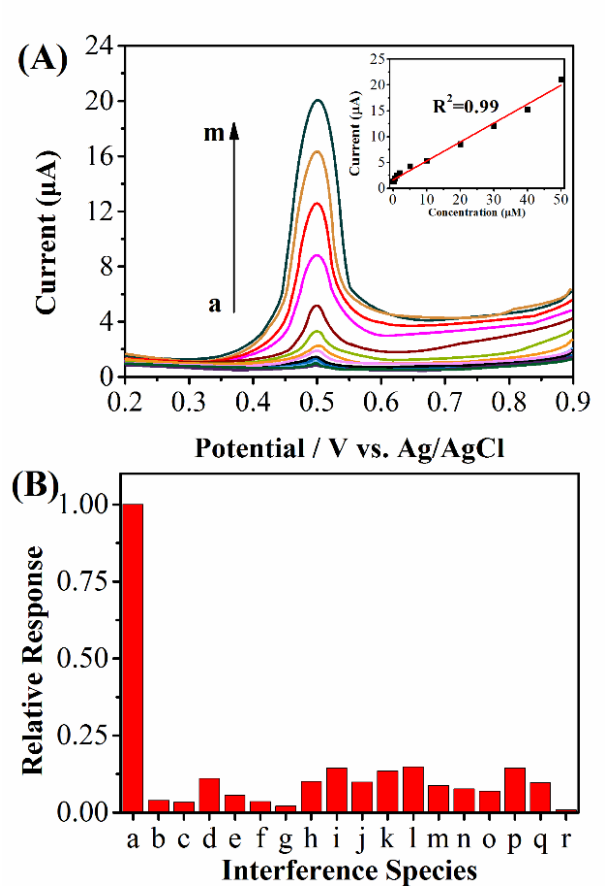

Figure 4. (A) DPV curves for BPA at β-CD/RGO/Au modified GCE with different concentrations of BPA (from a to m: 0.01, 0.05, 0.1, 0.2, 0.5, 1, 2, 5, 10, 20, 30, 40, 50 μM). (B) DPV peak current of interference species (from b to k: 1 μM of K^+, Zn^{2+}, Ca^{2+}, Mg^{2+}, Cu^{2+}, Na^+, Fe^{3+}, SO_4^{2-}, NO^{3-}, Cl^-. From l to r: 0.5 μM of hydroquinone, phenol, hydroxyphenol, 4-nitrophenol, 2,4-dinitrophenol, pyrocatechol and dioctyl hthalate) compared with (a) 0.01 μM BPA.

The effect of PBS pH on the detection of BPA using β-CD/RGO/Au modified GCE was also investigated. Figure 3E shows the CVs of oxidation BPA using β-CD/RGO/Au modified GCE at pH range from 3 to 11. As shown in Figure 3F, the oxidation peak current of BPA increased until pH reaches 7 and then conversely decreased. Therefore, pH 7.0 was selected as the optimum pH for the further studies. Figure 3F also displays a linear relationship between the oxidation peak potential and pH value. As the pH value increases, the oxidation potential shifts more positively, indicating that protons were directly involved in the oxidation process. The linear regression equation can be represented as: E_{pa} (V) = 0.0522 pH + 0.2749 (R^2 = 0.989). A slope of 52 mV per pH unit is close to the theoretical value of 57.6 mV per pH unit, indicating the electron transfer of BPA oxidation is

accompanied by an equal number of electrons and protons [17, 19, 73]. Therefore, the electrooxidation of BPA on β-CD/RGO/Au modified GCE is a two-electron and two-proton process. The proposed oxidation mechanism is illustrated in Figure S3.

Differential pulse voltammetric (DPV, scan range: 0.2−0.9 V, amplitude: 50 mV) was used for detecting BPA. Figure 4A shows the DPV responses for various concentrations of BPA at β-CD/RGO/Au modified GCE. The oxidation currents gradually increase followed with the BPA concentration increasing from 0.01 to 50 μM. The insert of Figure 4A demonstrates that the current response of β-CD/RGO/Au modified GCE is linearly related to the concentrations of BPA. The obtained linear regression equation can be expressed as I (μA) = 0.3368C (μM) + 1.62 (R^2 = 0.9901). The detection limit for BPA is calculated to be 0.003 μM based on a signal-to-noise ratio of 3.

The effect of some interference species on the determination of BPA was also investigated under the optimum experimental conditions. As summarized in Figure 4B, 100-fold concentrations of inorganic ions of K^+, Zn^{2+}, Ca^{2+}, Mg^{2+}, Cu^{2+}, Na^+, Fe^{3+}, SO_4^{2-}, NO^{3-}, Cl^- and 20-fold concentrations of hydroquinone, phenol, hydroxyphenol, 4-nitrophenol, 2,4-dinitrophenol, pyrocatechol dioctyl hthalate have no influence on the signals of BPA with the deviation below 10%. These results indicate that β-CD/RGO/Au modified GCE owing a good selectivity for determining BPA.

3.3 Repeatability, stability and real sample analysis

The reproducibility of as-synthesized BPA sensor was tested by 20 successive measurements in PBS containing 10 μM BPA. The RSD values were found to be 2.5% for the analyte. The storage stability also was tested by storing the modified GCE in fridge for 4 weeks. The results show that the oxidation peak potential of BPA had no shift and the current response only showed 3.8% decrease compared with the original test. Therefore, the BPA sensor fabricated by β-CD/RGO/Au nanocomposite exhibited a satisfactory reproducibility and stability.

Table 1. Determination of BPA in river water, liquid milk, mineralized water bottle and PVC film.

Sample	Detected (μM)	Added (μM)	Found (μM)	Recovery (%)	RSD (%)
River water	0.11	1	1.09	98.2	3.55
Mineralized water bottle	0.32	1	1.39	105.3	4.32
Mineralized water	Not detected	3	2.97	99.0	0.74
PVC film	2.09	3	5.22	102.6	1.01

In order to evaluate the practical performance of the proposed sensor, the fabricated β-CD/RGO/Au modified GCE was used to determine BPA in river water, liquid milk, mineralized water bottle and PVC film. The sample preparation of mineralized water bottle and PVC film was according to the literature [34]. As shown in Table 1, the recovery for the determination of BPA was in the range

of 99.0–105.3%. Therefore, the proposed BPA sensor could be employed for practical determining BPA concentration in real samples.

4. CONCLUSIONS

To sum up, we demonstrated a novel electrochemical sensor for detection of BPA was fabricated based on β-CD/RGO/Au nanocomposite modified GCE. The β-CD/RGO/Au nanocomposite was prepared via a microwave heating method coupled with an electrodeposition approach. The synthesized nanocomposite was characterized by a series of techniques. Owing to the excellent conductivity of RGO, supramolecular recognition capability of β-CD and superior electrocatalytic activity of Au NPs, the constructed electrochemical sensor not only displayed an excellent electrocatalytic performance toward the oxidation of BPA with a wider linear range and lower detection limit, but also exhibited a well stability and repeatability. In practical application investigations, the proposed sensor showed good recoveries and could be applied to determine BPA in various samples. Therefore, β-CD/RGO/Au nanocomposite was a promising electrode modifier for determining BPA by electrochemical technique.

Acknowledgements
This work was funded by Tianjin Key Laboratory for Prevention and Control of Occupational and Environmental hazards Opening Fund (WHKF201504).

References

1. H. Sambe, K. Hoshina, K. Hosoya and J. Haginaka, *Journal of Chromatography A*, 1134 (2006) 16
2. H. Hiroi, O. Tsutsumi, M. Momoeda, Y. Takai, Y. Osuga and Y. Taketani, *Endocrine Journal*, 46 (1999) 773
3. S. Safe, *Toxicology*, 205 (2004) 3
4. S.H. Safe, *Environ. Health Perspect.*, 108 (2000) 487
5. L.N. Vandenberg, R. Hauser, M. Marcus, N. Olea and W.V. Welshons, *Reproductive Toxicology*, 24 (2007) 139
6. J. Sajiki and J. Yonekubo, *Environment International*, 30 (2004) 145
7. P. Devi, P. Chakraborty and D. Dasgupta, *J Biol Inorg Chem*, 14 (2009) 347
8. K. Inoue, K. Kato, Y. Yoshimura, T. Makino and H. Nakazawa, *Journal of Chromatography B: Biomedical Sciences and Applications*, 749 (2000) 17
9. Y. Watabe, T. Kondo, M. Morita, N. Tanaka, J. Haginaka and K. Hosoya, *Journal of Chromatography A*, 1032 (2004) 45
10. A. Ballesteros-Gómez, S. Rubio and D. Pérez-Bendito, *Journal of Chromatography A*, 1216 (2009) 530
11. C.-M. Chang, C.-C. Chou and M.-R. Lee, *Anal. Chim. Acta.*, 539 (2005) 41
12. M.C. Estévez, R. Galve, F. Sánchez-Baeza and M.P. Marco, *Anal. Chem.*, 77 (2005) 5283
13. H. Xu, H. Li, J. Xia, S. Yin, Z. Luo, L. Liu and L. Xu, *ACS applied materials & interfaces*, 3 (2010) 22
14. S.C. Cunha and J.O. Fernandes, *Talanta*, 83 (2010) 117

15. V. Becerra and J. Odermatt, *The Analyst*, 137 (2012) 2250
16. Y. Zhang, Y. Cheng, Y. Zhou, B. Li, W. Gu, X. Shi and Y. Xian, *Talanta*, 107 (2013) 211
17. W. Zhou, C. Sun, Y. Zhou, X. Yang and W. Yang, *Food Chemistry*, 158 (2014) 81
18. L. Zhou, J. Wang, D. Li and Y. Li, *Food Chemistry*, 162 (2014) 34
19. H. Yin, L. Cui, Q. Chen, W. Shi, S. Ai, L. Zhu and L. Lu, *Food Chemistry*, 125 (2011) 1097
20. M. Najafi, M.A. Khalilzadeh and H. Karimi-Maleh, *Food Chemistry*, 158 (2014) 125
21. L. Fu, G. Lai, B. Jia and A. Yu, *Electrocatalysis*, 6 (2015) 72
22. L. Fu, G. Lai and A. Yu, *RSC Advances*, 5 (2015) 76973
23. L. Fu, S. Yu, L. Thompson and A. Yu, *RSC Advances*, 5 (2015) 40111
24. L. Fu, Y. Zheng, Z. Fu, A. Wang and W. Cai, *Bull Mater Sci*, (2015) 1
25. L. Fu, Y. Zheng and A. Wang, *Int. J. Electrochem. Sci*, 10 (2015) 3518
26. L. Fu, Y. Zheng, A. Wang, W. Cai, B. Deng and Z. Zhang, *Arab J Sci Eng*, (2015) 1
27. L. Fu, Y. Zheng, A. Wang, W. Cai, Z. Fu and F. Peng, *Sensor Letters*, 13 (2015) 81
28. L. Fu, Y. Zheng, A. Wang, W. Cai and H. Lin, *Food chemistry*, 181 (2015) 127
29. L. Fu, Y.-H. Zheng and Z.-X. Fu, *Chemical Papers*, 69 (2015) 655
30. Y. Zheng, L. Fu, A. Wang and W. Cai, *Int. J. Electrochem. Sci*, 10 (2015) 3530
31. Y. Zheng, L. Fu, A. Wang, F. Peng, J. Yang and F. Han, *Sensor Letters*, 13 (2015) 878
32. Y. Zheng, A. Wang, H. Lin, L. Fu and W. Cai, *RSC Advances*, 5 (2015) 15425
33. E. Mazzotta, C. Malitesta and E. Margapoti, *Anal Bioanal Chem*, 405 (2013) 3587
34. Y. Lin, K. Liu, C. Liu, L. Yin, Q. Kang, L. Li and B. Li, *Electrochimica Acta*, 133 (2014) 492
35. X. Tu, L. Yan, X. Luo, S. Luo and Q. Xie, *Electroanalysis*, 21 (2009) 2491
36. L. Fu, G. Lai, P.J. Mahon, J. Wang, D. Zhu, B. Jia, F. Malherbe and A. Yu, *RSC Advances*, 4 (2014) 39645
37. L. Fu, J. Yong, G. Lai, T. Tamanna, S. Notley and A. Yu, *Materials and Manufacturing Processes*, 29 (2014) 1030
38. L. Fu and A. Yu, *Rev. Adv. Mater. Sci*, 36 (2014) 40
39. F. Wang, X. Cao, X. Ren and P. Irani, Detecting and leveraging finger orientation for interaction with direct-touch surfaces, Proceedings of the 22nd annual ACM symposium on User interface software and technology, ACM, Victoria, BC, Canada, 2009, pp. 23.
40. H. Yin, Y. Zhou, S. Ai, Q. Chen, X. Zhu, X. Liu and L. Zhu, *J. Hazard. Mater.*, 174 (2010) 236
41. A. Qurashi, J.A. Rather, K. De Wael, B. Merzougui, N. Tabet and M. Faiz, *The Analyst*, 138 (2013) 4764
42. V. Chauke, F. Matemadombo and T. Nyokong, *J. Hazard. Mater.*, 178 (2010) 180
43. K.S. Novoselov, A.K. Geim, S.V. Morozov, D. Jiang, Y. Zhang, S.V. Dubonos, I.V. Grigorieva and A.A. Firsov, *Science*, 306 (2004) 666
44. W. Feng, C. Liu, S. Lu, C. Zhang, X. Zhu, Y. Liang and J. Nan, *Microchim. Acta.*, (2014)
45. R. Freeman, T. Finder, L. Bahshi and I. Willner, *Nano Letters*, 9 (2009) 2073
46. M.V. Rekharsky and Y. Inoue, *Chemical Reviews*, 98 (1998) 1875
47. C. Shan, H. Yang, D. Han, Q. Zhang, A. Ivaska and L. Niu, *Biosensors and Bioelectronics*, 25 (2010) 1070
48. J.M. Pingarrón, P. YáñezSedeñoandA. González-Cortés, *Electrochimica Acta*, 53 (2008) 5848
49. A. Wang, H.P. Ng, Y. Xu, Y. Li, Y. Zheng, J. Yu, F. Han, F. Peng and L. Fu, *Journal of Nanomaterials*, 2014 (2014) Article ID 451232
50. H. Cheng, G. Lai, L. Fu, H. Zhang and A. Yu, *Biosensors and Bioelectronics*, 71 (2015) 353
51. G. Lai, H. Cheng, C. Yin, L. Fu and A. Yu, *Electroanalysis*, (2015)
52. W.S. Hummers and R.E. Offeman, *Journal of the American Chemical Society*, 80 (1958) 1339
53. T. Gan and S. Hu, *Microchim. Acta.*, 175 (2011) 1
54. W. Liu, C. Li, Y. Gu, L. Tang, Z. Zhang and M. Yang, *Electroanalysis*, (2013) 2367
55. J. Zhang, H. Yang, G. Shen, P. Cheng, J. Zhang and S. Guo, *Chemical Communications*, 46 (2010) 1112

56. M. Ahmad, E. Ahmed, Z.L. Hong, J.F. Xu, N.R. Khalid, A. Elhissi and W. Ahmed, *Appl. Surf. Sci.*, 274 (2013) 273
57. X. Li, Q. Wang, Y. Zhao, W. Wu, J. Chen and H. Meng, *Journal of colloid and interface science*, 411 (2013) 69
58. X. Ye, Y. Du, D. Lu and C. Wang, *Anal. Chim. Acta.*, 779 (2013) 22
59. W. Zhang, M. Chen, X. Gong and G. Diao, *Carbon*, 61 (2013) 154
60. H. Liu, C. Liu, X. Yang, S. Zeng, Y. Xiong and W. Xu, *Anal. Chim. Acta.*, 628 (2008) 87
61. Z.-J. Fan, W. Kai, J. Yan, T. Wei, L.-J. Zhi, J. Feng, Y.-m. Ren, L.-P. Song and F. Wei, *ACS Nano*, 5 (2010) 191
62. X. Li, Q. Wang, Y. Zhao, W. Wu, J. Chen and H. Meng, *Journal of colloid and interface science*, 411 (2013) 69
63. S. Kamada, H. Nomoto, K. Fukuda, T. Fukawa, H. Shirai and M. Kimura, *Colloid Polym Sci*, 289 (2011) 925
64. J.I. Paredes, S. Villar-Rodil, A. Martínez-Alonso and J.M.D. Tascón, *Langmuir*, 24 (2008) 10560
65. X.C. Lv and J. Weng, *Scientific reports*, 3 (2013)
66. T. Nakajima, A. Mabuchi and R. Hagiwara, *Carbon*, 26 (1988) 357
67. D. Chen, L. Li and L. Guo, *Nanotechnology*, 22 (2011)
68. J. Yang, S.-E. Kim, M. Cho, I.-K. Yoo, W.-S. Choe and Y. Lee, *Biosensors and Bioelectronics*, 61 (2014) 38
69. E. Laviron, *J. Electroanal. Chem.*, 101 (1979) 19
70. E. Laviron, *J. Electroanal. Chem.*, 52 (1974) 355
71. K.-J. Huang, Y.-J. Liu, Y.-M. Liu andL.-L. Wang, *J. Hazard. Mater.*, 276 (2014) 207
72. H. Fan, Y. Li, D. Wu, H. Ma, K. Mao, D. Fan, B. Du, H. Li and Q. Wei, *Anal. Chim. Acta.*, 711 (2012) 24
73. H. Yin, Q. Zhang, Y. Zhou, Q. Ma, T. liu, L. Zhu and S. Ai, *Electrochimica Acta*, 56 (2011) 2748